EARTHQUAKE ENGINEERING AND STRUCTURAL DYNAMICS, VOL. 24, 1527–1539 (1995)

STATISTICAL ANALYSIS OF PEAKS AND DIRECTIVITY OF EARTHQUAKE GROUND MOTION

MEHEDI A. ANSARY*, FUMIO YAMAZAKI† AND TSUNEO KATAYAMA‡
Institute of Industrial Science, The University of Tokyo, 7-22-1 Roppongi, Minato-ku, Tokyo 106, Japan

SUMMARY

Conversion factors are useful for attenuation and damage estimation relationships. These factors among different definitions of peaks (i.e. larger, average and resultant) for peak ground motion indices and acceleration response spectrum were investigated. A large number of horizontal acceleration records recorded at 76 free-field sites of the Japan Meteorological Agency were used in this study. Two orthogonal horizontal components were combined in the time domain to get the maximum resultant peak ground motion indices and acceleration response spectrum in the horizontal plane. From the analysis, the means of the larger/resultant ratio were found to be 0·934 for acceleration, 0·926 for velocity, and 0·913 for displacement. A similar decreasing trend was observed for the means of the average/resultant ratio of the ground motion indices and acceleration response spectrum. The directivity of peak ground motion indices was also examined. It was found that the peak ground motion is more likely to occur in the transverse direction than in other directions. This trend is more prominent in the long-period contents of ground motion.

INTRODUCTION

One of the characteristics of earthquake ground motions of considerable interest in design is the peak values of horizontal ground motions developed at a specific site during an earthquake. Three principal parameters are generally considered, i.e. peak ground acceleration (PGA), peak ground velocity (PGV) and peak ground displacement (PGD). Peak ground motions are widely used as an index of the intensity of ground shaking. However, these parameters do not necessarily represent all the features of ground motions because damage to structures is also related to the frequency contents and the duration of strong motion. The PGA, PGV and PGD have been shown[1,2] to be correlated to the damage of short-period, intermediate-period, and long-period structures, respectively. On the other hand, earthquake response spectra may be more relevant parameters of the characteristics of ground shaking because these account for both the frequency characteristics and the intensity of ground motion.

Most of the previous studies of Japanese strong motion records used data provided by the SMAC-type accelerographs. This study used a new set of data recorded by the JMA-87 type accelerographs of the Japan Meteorological Agency (JMA). SMAC accelerographs are mechanical type and these suppress high frequencies. On the other hand, the new JMA-87 accelerographs are electromagnetic type and have a flat sensitivity from 0·05 to 10 Hz and can measure accelerations from 30×10^{-3} to 980 cm/s^2 for periods from 1 s to 10 min.[3] Data supplied by JMA from these accelerographs do not need instrument correction.

Generally, in the analysis of peak horizontal ground motions, either only the larger[4,5] or the average[6,7] of the two components or both[8] are used. However, the two horizontal components of ground motion provided by an instrument represent only the shaking in the direction along which the instrument is set up. Since the axis of the structure to which the seismic force is applied is generally different from the direction of the instrument, it is more reasonable from the conservative design viewpoint to consider the maximum

* Graduate Student
† Associate Professor
‡ Professor

CCC 0098–8897/95/111527–13

Received 31 August 1994
Revised 5 June 1995

ground motion on the horizontal plane obtained by combining the two horizontal components in the time domain.

In this study, a statistical analysis is conducted for the peak horizontal ground motions (PGA, PGV and PGD) and acceleration response spectrum. The average and the larger of the two components of the ground motion indices are compared with the resultant of the two horizontal components. The conversion factors for different definitions of peaks are then obtained. Directivities of the peak horizontal ground motions are also investigated to examine the distribution of peaks in the horizontal plane with respect to the epicentre.

STRONG MOTION DATA AND ANALYSIS TECHNIQUE

A total of 684 sets of two horizontal components, i.e. 1368 horizontal acceleration records from 201 earthquakes were used in this study. Earthquakes with a magnitude greater than or equal to 4·0 and horizontal acceleration components having a PGA of 5 cm/s^2 or greater in any direction were selected for the analysis. The ground motions of these earthquakes were recorded at 76 free-field sites of the JMA from 1 August 1988 to 30 August 1992. Records from recent earthquakes like the 15 January 1993 Kushiro-Oki earthquake[9] ($M_{JMA} = 7{\cdot}8$), the 7 February 1993 Noto Peninsula earthquake[10] ($M_{JMA} = 6{\cdot}6$), and 12 July 1993 Hokkaido Nansai-Oki earthquake[11] ($M_{JMA} = 7{\cdot}8$) were also included. Among the records about 70 per cent were recorded either on hard soils or rock and the remaining 30 per cent were recorded on medium to soft soil. Figures 1(a) and 1(b) show distribution of strong motion data in terms of earthquake magnitude and hypocentral distance.

The velocities and displacements were obtained from the acceleration records by integration in the frequency domain. To remove long-period noise, a cosine filter with a lower cut-off frequency between 0·01 and 0·05 Hz was employed for most of the records. However, this filter could not remove long-period noise for several records. For such cases, a cosine filter with a lower cut-off frequency between 0·10 and 0·12 Hz was used.

Figures 2(a)–(c) show the distributions of the resultant PGA, PGV and PGD of the 684 data. From these figures, we can conclude that most of the values lie below 100 cm/s^2 for acceleration, 8 cm/s for velocity and 2 cm for displacement. The exceptional case is the record of the Kushiro–Oki earthquake at Kushiro station (see Figure 11), whose resultant PGA is 1024 cm/s^2; resultant PGV, 71·3 cm/s; and resultant PGD, 8·2 cm.

Definition of peaks

Two peak values, i.e. the larger, L, and the average, A, used in this study are defined as

$$L = \mathrm{Max}\,[\mathrm{Max}[\,|x(t)|\,]_{\mathrm{for}\,t}, \mathrm{Max}[\,|y(t)|\,]_{\mathrm{for}\,t}] \tag{1}$$

$$A = [\mathrm{Max}[\,|x(t)|\,]_{\mathrm{for}\,t} + \mathrm{Max}[\,|y(t)|\,]_{\mathrm{for}\,t}]/2 \tag{2}$$

in which $x(t)$ and $y(t)$ are the two orthogonal components of a record. These two horizontal orthogonal components of the ground motion are combined on the horizontal plane to get the resultant value, $r(\theta, t)$. The resultant is calculated for each directional angle θ from 0 to 2π by

$$r(\theta, t) = x(t)\cos\theta + y(t)\sin\theta \tag{3}$$

and

$$r_{\max}(\theta) = \mathrm{Max}[\,|r(\theta, t)|\,]_{\mathrm{for}\,t} \tag{4}$$

R, $\bar{A}$ and $R_{\min}$ are the largest, average, and the smallest among all the $r_{\max}(\theta)$ values, respectively, as given by

$$R = \mathrm{Max}[r_{\max}(\theta)]_{\mathrm{for}\,\theta} \tag{5}$$

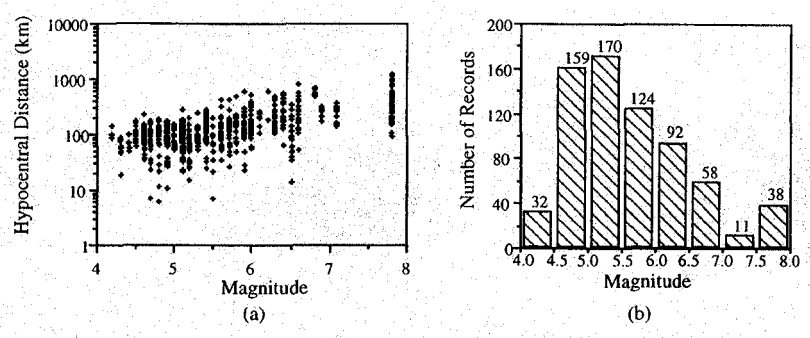

Figure 1. Distribution of strong motion data in terms of earthquake magnitude and hypocentral distance: (a) magnitude-hypocentral distance; (b) histogram of magnitude

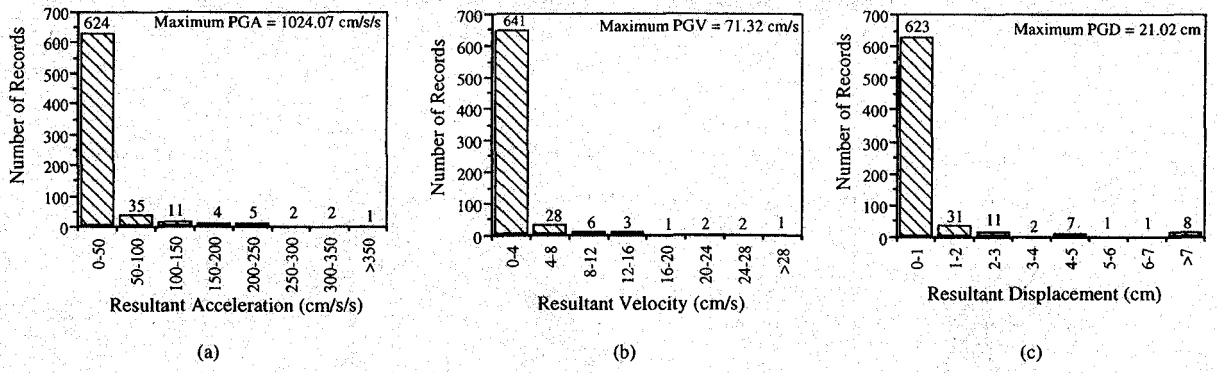

Figure 2. Distribution of the resultant peak ground motions: (a) PGA; (b) PGV; (c) PGD

$$\bar{A} = \frac{1}{2\pi} \int_0^{2\pi} r_{\max}(\theta)\, \mathrm{d}\theta \tag{6}$$

$$R_{\min} = \mathrm{Min}[r_{\max}(\theta)]_{\text{for } \theta} \tag{7}$$

Analysis of an earthquake record

The record of the 1993 Hokkaido–Nansei–Oki earthquake at Suttsu station (see Figure 11) having a resultant PGA = 216·6 cm/s^2, PGV = 14·3 cm/s and PGD = 7·8 cm was selected to demonstrate the nature of the particle trace and analysis technique used in this study. Figure 3 shows the particle traces of acceleration, velocity, and displacement of the record for the time window of 5–15 s on the horizontal plane. The orbits look quite different: displacement shows a predominant direction while acceleration and velocity do not. Their peaks occur at different times and directions. These observations indicate that the directivity of earthquake ground motion is frequency-dependent.

Figure 4 shows the traces of the acceleration response spectrum of the same record on the horizontal plane for different structural periods. The figure indicates that peaks and directions of acceleration response change with structural period. The short-period orbit is similar to acceleration orbit, i.e. no predominant direction exists, while the long-period orbit is similar to the displacement orbit, i.e. a predominant direction exists. The intermediate-period orbit lies between these two cases.

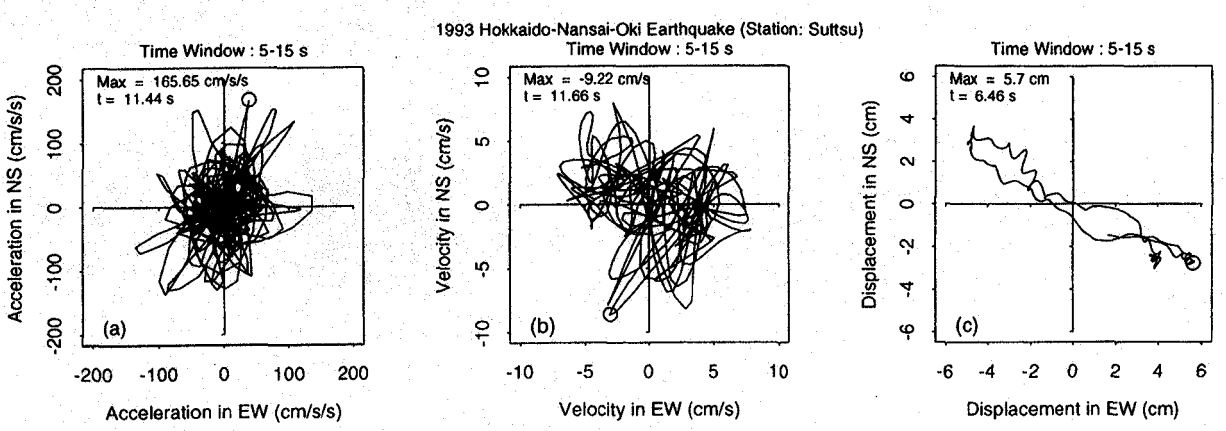

Figure 3. Particle traces of acceleration, velocity and displacement of an earthquake record

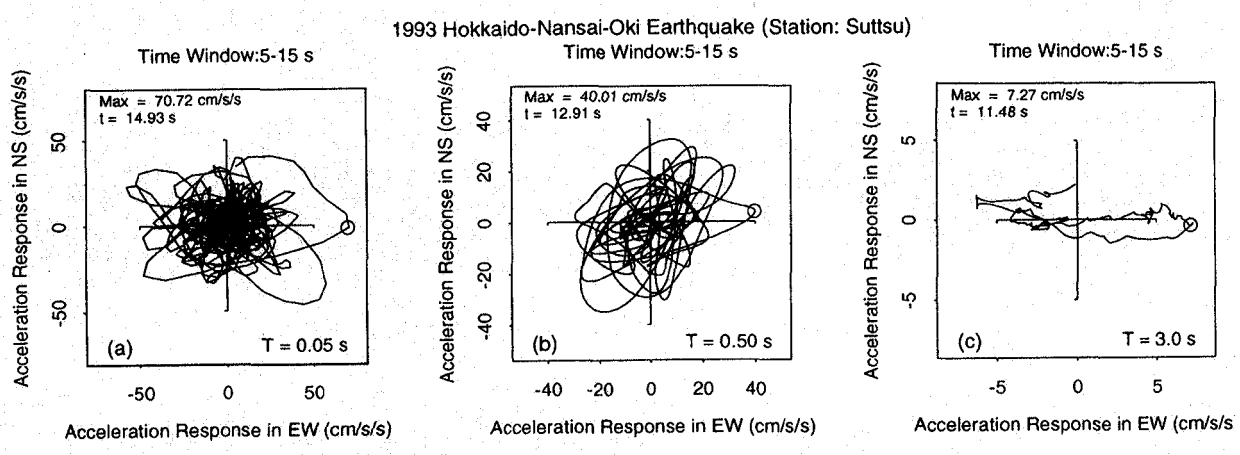

Figure 4. Particle traces of acceleration response spectrum of an earthquake record for different periods

The envelope (i.e. the trace of $r_{max}(\theta)/R$ ratio) of the earthquake record at Suttsu station for the full time window is shown in Figure 5. The maximum resultant in any particular direction is calculated by equation (4) for either acceleration, velocity or displacement record. α is the angle between R [equation (5)] and R_{min} [equation (7)] as shown in Figure 5. The cross and the circular symbols in the figure represent the position of R and R_{min}, respectively. In this particular record, R_{min}/R, $\bar{A}/R$ and α are 0·815, 0·923, and 60° for acceleration; 0·730, 0·875, and 61° for velocity; 0·301, 0·714, and 88° for displacement. For low values of R_{min}/R, α lies around 90° as can be observed for the displacement record. For high values of R_{min}/R, the angle deviates away from 90° as can be observed from the acceleration and velocity records. The decreasing value of the R_{min}/R ratio from acceleration to displacement also substantiates that it may be a key parameter that can indicate the presence of predominant direction of a record. In the presence of predominant direction, R and R_{min} may have some relation with the major and intermediate principal axes,[12,13] where the principal axes for earthquake ground motions are defined as those along which the component variances have maximum and intermediate values and the covariances are equal to zero.

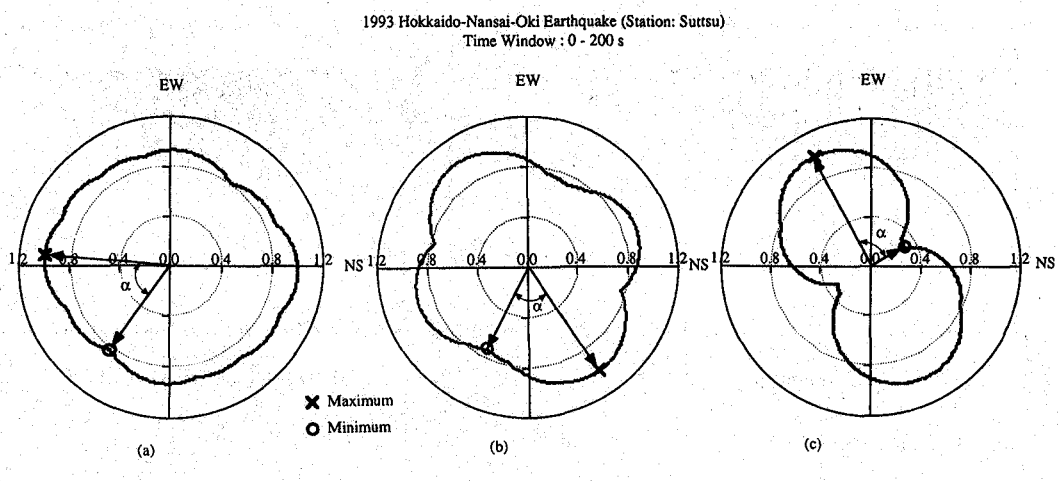

Figure 5. Trace of $r_{max}(\theta)/R$ ratio for acceleration, velocity and displacement of an earthquake record: (a) acceleration; (b) velocity; (c) displacement

ANALYSIS OF PEAK GROUND MOTION

The resultant, the average, and the larger values of the two horizontal motions were determined for all the 684 data. Then the larger/resultant, L/R, ratio was calculated and plotted with respect to magnitude and hypocentral distance in Figure 6. This figure shows that the L/R ratio for PGA is almost independent of magnitude and hypocentral distance. A similar trend can also be observed for PGV and PGD.

Table I shows the mean, the standard deviation, the maximum, and the minimum of L/R and A/R ratios for PGA, PGV and PGD. Between the two sets of values, the L/R ratio has higher mean value and smaller standard deviation compared to the average/resultant (A/R) ratio.

Table II compares the R/L ratio by Kawashima *et al.*[14] and by this study, Kawashima *et al.* showed that the maximum peak ground motions (PGA, PGV and PGD) determined by the combination of two horizontal components are about 8 per cent greater in magnitude than the larger of the two horizontal components. However, in this study, the resultant PGA is about 8 per cent greater; resultant PGV, about 9 per cent greater; and resultant PGD, about 10 per cent greater in magnitude than the larger of the two horizontal components. The variation in the R/L ratios among PGA, PGV and PGD may be explained by the fact that acceleration is more isotropic than velocity and displacement: the acceleration orbit is close to a circle in the horizontal plane as shown in Figures 3 and 5. Since high-frequency contents are spatially less coherent than low-frequency contents,[15-17] the acceleration orbit may show less directivity than the velocity and displacement orbits. On the other hand, Kawashima's analysis, which used mostly data provided by SMAC-type accelerographs, has shown almost stable R/L ratios for PGA, PGV and PGD. This result may be attributed to the low sensitivity of the SMAC accelerograph in the high-frequency range although an instrument correction was applied.

Figure 7 shows the histogram and the cumulative distribution of the L/R ratio of PGA. Theoretically, the L/R ratio should lie from 0·707 to 1·0. The cumulative distribution of the L/R ratio is similar to a trigonometric distribution. When the larger value is the larger of the two orthogonal horizontal components of the maximum resultant, the ratio between any of the two components and the resultant is either cosine or sine value. However, in this analysis, a larger [equation (1)] value is the largest among the time histories of two components. Thus, the distribution of the L/R ratio does not match the trigonometric distribution although the trend of the distribution is similar.

A similar tendency to the L/R ratio can be seen for the A/R ratio in Table I, i.e. the ratio for PGD is lower compared to those for PGA and PGV. To check this general idea, the mean, the standard deviation, the

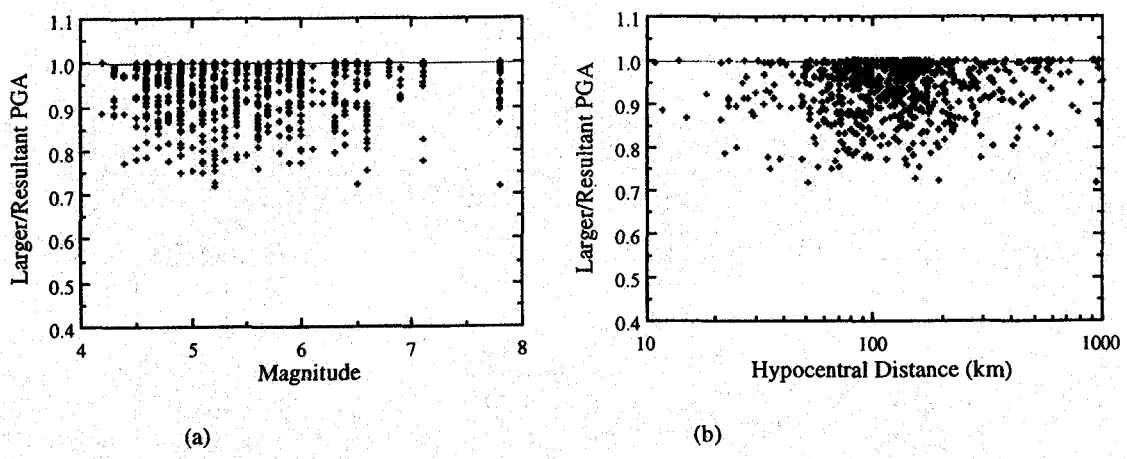

Figure 6. Distribution of larger/resultant (L/R) ratio of PGA with respect to magnitude and hypocentral distance: (a) magnitude-L/R ratio; (b) hypocentral distance-L/R ratio

Table I. Mean, standard deviation, maximum and minimum of the ratios (L/R and A/R) of ground motion indices

Ratio	Index	Mean	Standard deviation	Maximum	Minimum
Larger/resultant (L/R)	PGA	0·934	0·063	1·000	0·717
	PGV	0·926	0·065	1·000	0·714
	PGD	0·913	0·075	1·000	0·707
Average/resultant (A/R)	PGA	0·833	0·075	0·992	0·501
	PGV	0·819	0·078	0·987	0·505
	PGD	0·782	0·082	0·983	0·506

Table II. Comparison between the resultant/larger (R/L) ratios by Kawashima *et al.*[14] and by this study

Index	Kawashima *et al.*		This study	
	Mean	Standard deviation	Mean	Standard deviation
PGA	1·086	0·079	1·076	0·079
PGV	1·083	0·089	1·085	0·082
PGD	1·077	0·075	1·103	0·097

maximum and the minimum of $\bar{A}/R$ and R_{min}/R for the 684 data were calculated and shown in Tables III and IV, respectively. It is observed that the mean values of $\bar{A}/R$ in Table III and A/R in Table I are almost the same, although the definitions of $\bar{A}$ [equation (6)] and A [equation (2)] are different. The standard deviation of $\bar{A}/R$ is found to be smaller than those of A/R ratio. This can be explained by the fact that the $\bar{A}/R$ ratio has a narrower range of distribution since it is the average for all the directions. On the other hand, the A/R ratio

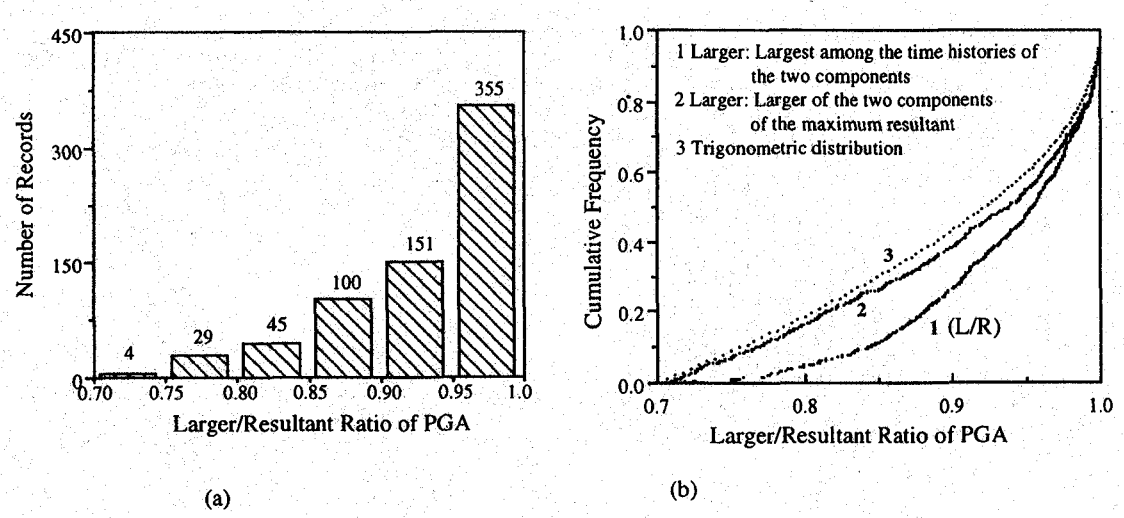

Figure 7. Distribution of larger/resultant (L/R) ratios of PGA: (a) histogram of L/R ratio; (b) cumulative frequencies of various ratios

Table III. Mean, standard deviation, maximum and minimum of the $\bar{A}/R$ ratio of ground motion indices

Index	Mean	Standard deviation	Maximum	Minimum
PGA	0·830	0·062	0·967	0·637
PGV	0·819	0·065	0·957	0·637
PGD	0·787	0·071	0·962	0·637

Table IV. Mean, standard deviation, maximum and minimum of the R_{min}/R ratio of ground motion indices

Index	Mean	Standard deviation	Maximum	Minimum
PGA	0·622	0·132	0·885	0·001
PGV	0·600	0·140	0·873	0·010
PGD	0·513	0·166	0·876	0·013

is the average for two particular directions. The maximum and minimum values for the ratios are also consistent with this explanation.

Figure 8 shows the histogram and the cumulative distribution of the average/resultant (A/R and $\bar{A}/R$) ratio of PGA. Theoretically, the average/resultant ratio should lie from 0·5 to 1·0. The cumulative distributions of the A/R and $\bar{A}/R$ ratios show some kind of bounded distribution. However, the slope of the cumulative distribution of the $\bar{A}/R$ ratio is higher. This is due to the narrower distribution range of $\bar{A}/R$.

Table IV shows that the R_{min}/R ratio decreases from PGA, PGV, PGD. Hence, in general, it can be concluded that smaller R_{min}/R values indicate predominant direction. Figure 9 shows the distributions of R_{min}/R ratio and angle between R and $R_{min}(\alpha)$ for PGA. The R_{min}/R ratio shows high frequency from 0·5 to 0·8 (77 per cent of all the records) with the highest frequency from 0·6 and 0·7. The distribution of α looks almost uniform.

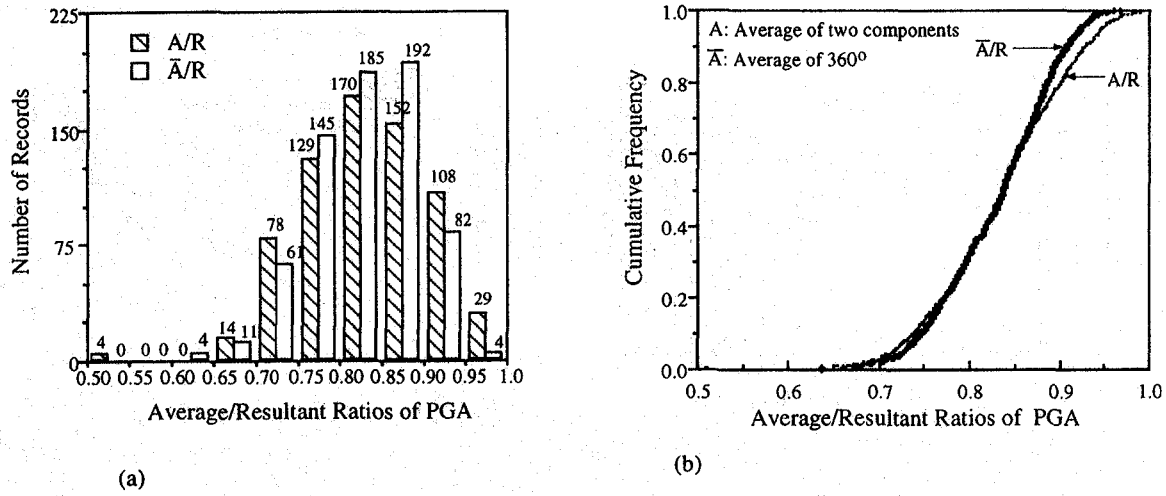

Figure 8. Distribution of average/resultant ratios (A/R and $\bar{A}/R$) of PGA: (a) histogram of A/R and $\bar{A}/R$ ratios; (b) cumulative frequency of A/R and $\bar{A}/R$ ratios

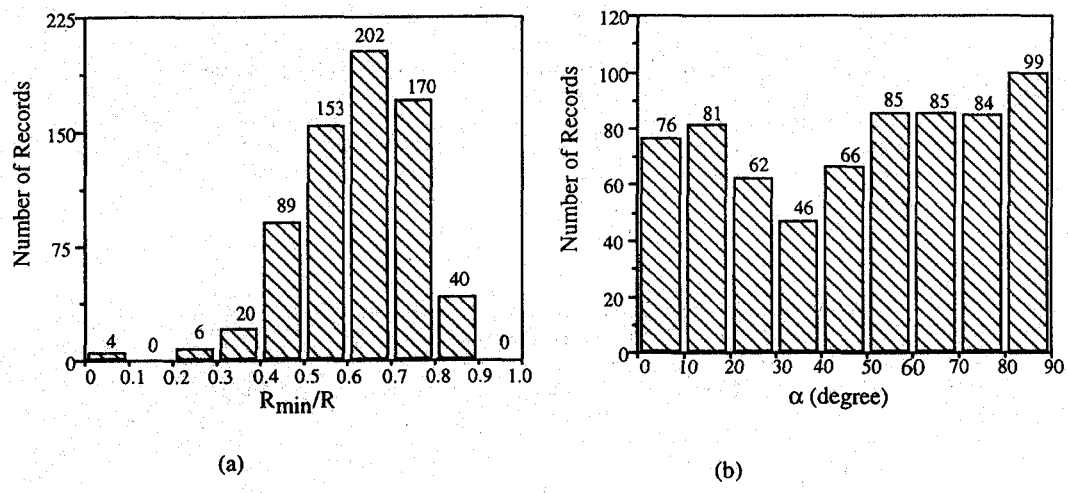

Figure 9. Distribution of R_{min}/R and angle between R and R_{min} for the acceleration records: (a) R_{min}/R ratio; (b) angle between R and R_{min}

Campbell[6] reported that the larger of the two horizontal components of PGA is about 12 per cent greater in magnitude than the average of the two horizontal components. In this study, the larger of the two horizontal components of PGA is about 11 per cent; of PGV, about 13 per cent; and of PGD, about 17 per cent greater in magnitude than the average of the two horizontal components. This can also be attributed to the fact that acceleration is more isotropic than velocity and displacement.

ANALYSIS OF ACCELERATION RESPONSE SPECTRUM

The response of a single-degree-of-freedom (SDOF) system was first calculated assuming a damping ratio (= 0·05) and structural periods (15 periods from 0·05 to 10 s) for two horizontal components. The

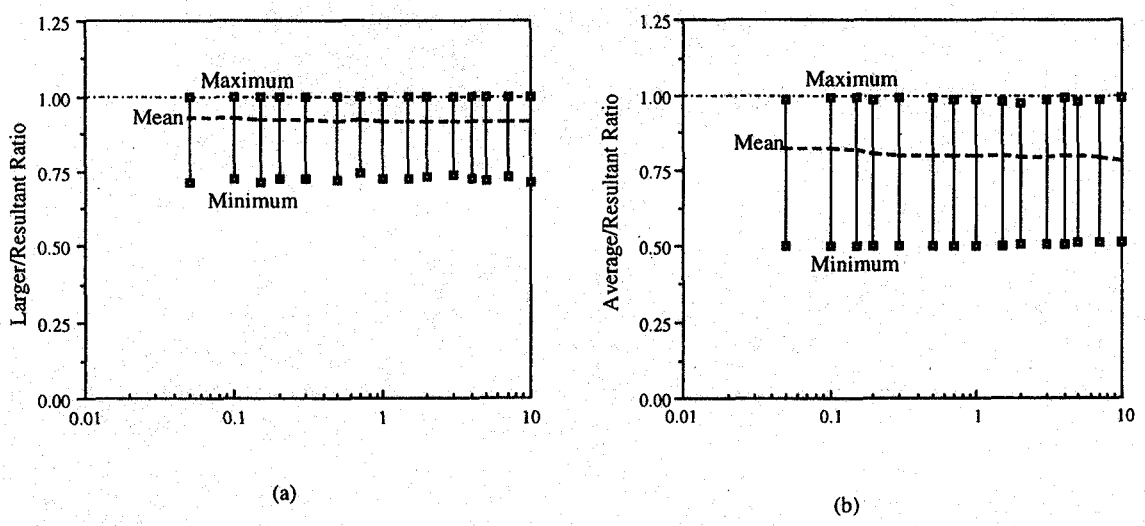

Figure 10. Variation of larger/resultant (L/R) and average/resultant (A/R) ratios of acceleration response spectrum with respect to the period: (a) L/R ratio; (b) A/R ratio

resultant, the average, and the larger values of responses for the two horizontal components were then calculated.

Response of a SDOF structure depends largely on its period. In Figure 10, the mean, maximum and minimum of the L/R and A/R ratios for the 684 sets of records are plotted with respect to the structural period. From this figure, however it is difficult to see the trend of the L/R and A/R ratios with respect to the period. Hence, the mean, standard deviation, maximum, and minimum of these ratios are tabulated in Tables V and VI. From these tables, it can be concluded that, in general, the mean of both the L/R and A/R ratios decreases and the standard deviation increases with an increase in structural period. The reason for these trends lies in the fact that the acceleration response spectrum at short period is more isotropic than at the intermediate and long periods. This is similar to the trend observed for PGA, PGV, and PGD. Some researchers[18,19] established that, in general, the short period portion of the response spectrum can be taken as being proportional to PGA; the intermediate portion, about 0·3–2 s to PGV; and the long-period portion to PGD. This fact is clearly visible if we compare the mean and standard deviation of the L/R and A/R ratios from Tables I, V, and VI. The mean and standard deviation of the A/R ratio for the peak ground motion indices vary from 0·782 to 0·833 and 0·075 to 0·082 (Table I), respectively. Those values for acceleration response spectrum with variable structural period vary from 0·793 to 0·838 and 0·074 to 0·081 (Table VI), respectively. Similar coincidence of means and standard deviations can also be seen in the L/R ratios in Tables I and V.

DIRECTIVITY ANALYSIS

The directivity of strong ground motion has been studied by several researchers.[20–23] In most of these studies, directivity refers to the azimuthal variations in the ground motion due to rupture direction. The reference cited either considers rupture towards the recording site or away from the recording site. On the other hand, in this study directivity is used to mean the difference in the ground motion as a function of source azimuth. Here, directivities of the peak horizontal ground motions are investigated to examine the distribution of peaks in the horizontal plane with respect to the epicenter.

As initial steps to examine the directivity, the distribution of the radial axis (i.e. the epicentre to the observation site) for all the 684 data and the map of recording stations and epicentres were plotted (see

Table V. Mean, standard deviation, maximum and minimum of larger/resultant (L/R) ratios of acceleration response spectrum with 5% damping

Period(s)	Mean	Standard deviation	Maximum	Minimum
0·05	0·936	0·062	1·000	0·711
0·10	0·937	0·061	1·000	0·724
0·15	0·931	0·066	1·000	0·714
0·20	0·929	0·064	1·000	0·724
0·30	0·932	0·063	1·000	0·724
0·50	0·924	0·067	1·000	0·716
0·70	0·929	0·064	1·000	0·742
1·0	0.928	0·065	1·000	0·723
1.5	0·925	0·065	1·000	0·723
2·0	0·926	0·068	1·000	0·726
3·0	0·926	0·067	1·000	0·734
4·0	0·924	0·069	1·000	0·724
5·0	0·927	0·068	1·000	0·716
7·0	0·927	0·068	1·000	0·728
10·0	0·926	0·069	1·000	0·709

Table VI. Mean, standard deviation, maximum and minimum of average/resultant (A/R) ratios of acceleration response spectrum with 5% damping

Period(s)	Mean	Standard deviation	Maximum	Minimum
0·05	0·838	0·074	0·988	0·501
0·10	0·833	0·075	0·991	0·501
0·15	0·830	0·077	0·993	0·502
0·20	0·819	0·077	0·990	0·502
0·30	0·810	0·076	0·993	0·502
0·50	0·809	0·077	0·994	0·502
0·70	0·811	0·077	0·988	0·502
1·0	0·810	0·077	0·986	0·503
1.5	0·810	0·079	0·981	0·503
2·0	0·807	0·078	0·977	0·505
3·0	0·805	0·078	0·989	0·507
4·0	0·808	0·080	0·992	0·508
5·0	0·810	0·079	0·982	0·510
7·0	0·803	0·078	0·986	0·511
10·0	0·793	0·081	0·992	0·514

Figure 11). In the figure, the horizontal plane is divided into 16 equal angles of 22·5° to show the direction of the radial axis. The density of records in the northeastern direction is higher compared to those of the other directions since a large number of epicentres are situated in the northeastern coast of Japan. Hence, this figure simply indicates the relationship between the epicentres and the observation stations.

Next, the angles from the north to the maximum resultant ground motions (θ in Figure 12(d)) were calculated. Figures 12(a)–(c) show the distributions of the maximum resultant ground motions with respect to the radial axis ($\theta - \theta_e$ in Figure 12(d)). The number beside the symbol in the figure denotes the number of earthquake records in each angular division. The thick line denotes the average frequency for each division.

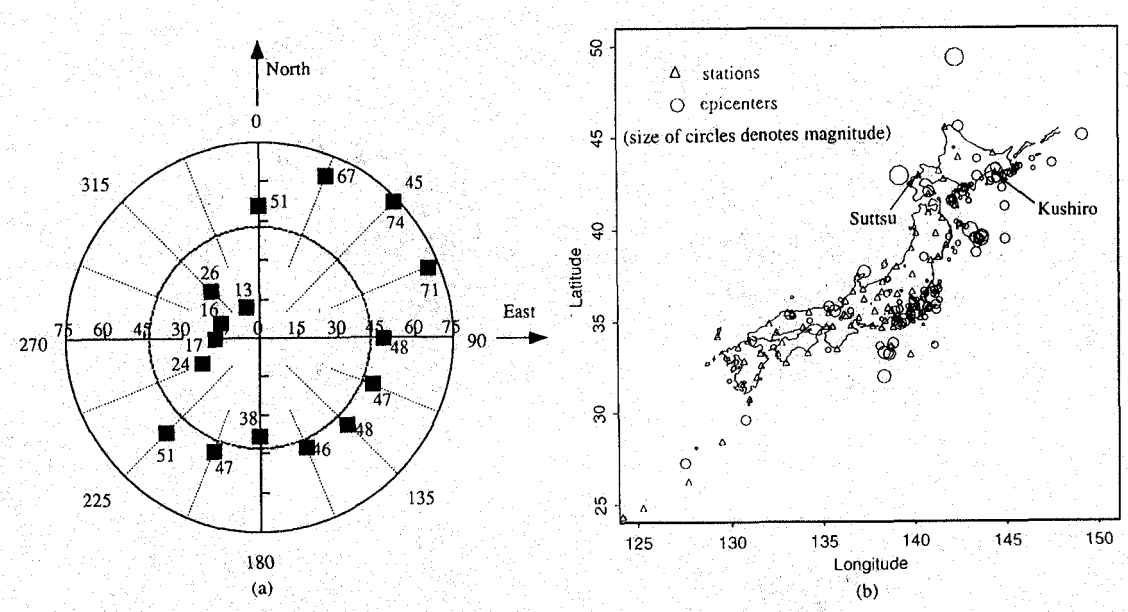

Figure 11. Distribution of the radial axis from the north (a) and map of the locations of JMA recording stations and earthquake epicentres used in this study (b)

To examine the directivity in a particular direction, a statistical hypothesis was tested using the two-tailed *t*-test with 95 per cent confidence level. The null hypothesis is uniform distribution of the peaks in each angular division. In the hypothesis test, all the records were classified into 8 groups. Each group contains the records of an angular division and the records of the opposite angular division. Failure of the test for any group indicates the failure of the uniformity assumption. In this analysis, all the ground motion indices failed the test. Figure 12 indicates that the frequency of PGA is high along the transverse axis and in another direction almost orthogonal to it. The frequencies of PGV and PGD are high along the transverse axis although it is more prominent for PGD. Hence, it can be concluded that the peak ground motion is more likely to occur in the transverse direction than in other directions and that this trend is more prominent in the long-period contents of ground motion. This conclusion is based on Japanese strong motion data which consists mostly of far-field records.

CONCLUSION

The results of the statistical analysis of peak ground motion and acceleration response spectrum for the 684 sets of horizontal strong motion recorded by the JMA-87 type accelerograph at 78 free-field sites of JMA were presented. The larger/resultant and the average/resultant ratios for this data set were derived by combining two horizontal components in the time domain. The larger/resultant motion is found to change depending on the ground motion index: 0·934 for PGA, 0·926 for PGV and 0·913 for PGD. Although, this observation contradicts the result of Kawashima *et al.*,[14] such trends can be explained by the shapes of the traces of ground motions: displacement shows stronger directivity than velocity and acceleration, and acceleration has more uniform peak values for all the directions on the horizontal plane. The average/resultant ratio showed a similar trend to the larger/resultant ratio, i.e. the ratio for PGA is the largest and that for PGD is the smallest.

It is observed that the larger/resultant and average/resultant ratios for acceleration response spectrum decrease with an increase in structural periods. The means and standard deviations of both the ratio for

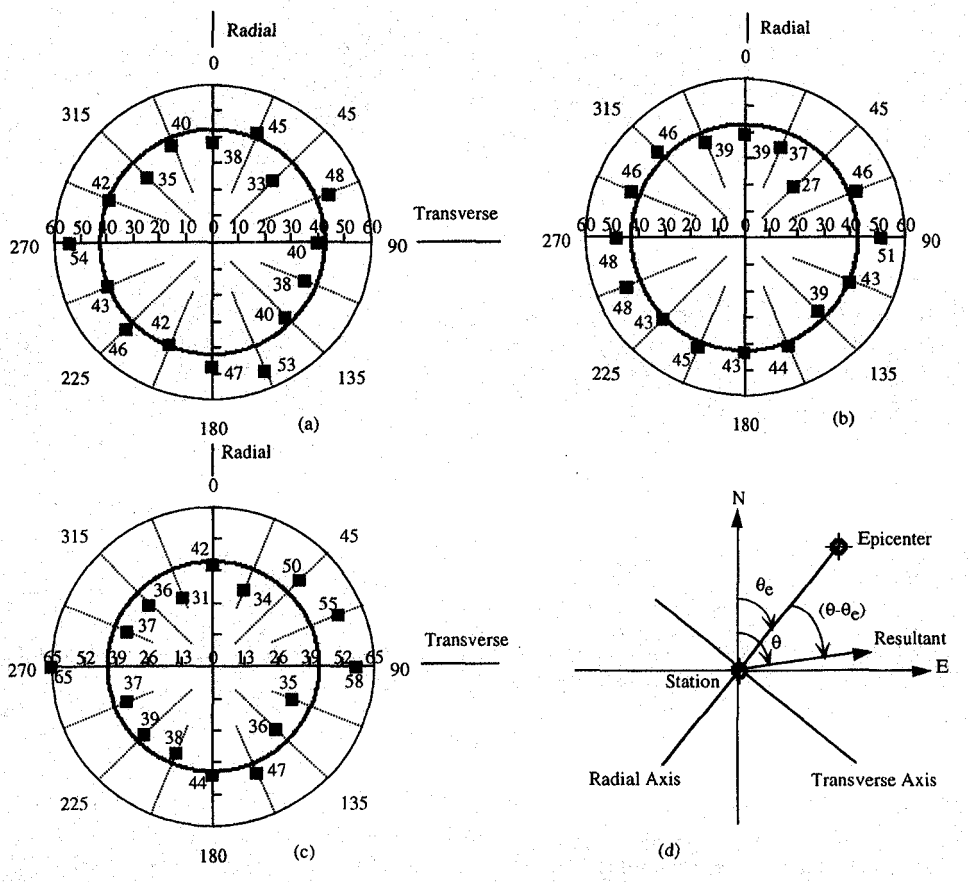

Figure 12. Distribution of the maximum resultant ground motion indices with respect to the radial axis: (a) PGA; (b) PGV; (c) PGD; (d) definition of angles

PGA, PGV and PGD correspond to the means and standard deviations of acceleration response spectrum from short to long periods.

Directivity of the resultant peaks was also examined for the same Japanese strong motion data set. It was found that the peak ground motion is more likely to occur in the transverse direction than in other directions and that this trend is more prominent in the long-period contents of ground motion.

ACKNOWLEDGEMENTS

The authors wish to thank Prof. G. B. Warburton and three other reviewers of this paper for their constructive comments. The first author also wishes to thank Dr. G. Molas, Post Doctoral Fellow, Institute of Industrial Science, University of Tokyo for sharing his knowledge.

REFERENCES

1. Y. Ando, F. Yamazaki and T. Katayama, 'Damage estimation of structures based on indices of earthquake ground motion', *Proc. 8th Japan earthquake eng. symp.* I, 715–720 (1990) (in Japanese).
2. K. Matsumura, 'On the intensity measure of strong motions related to structural failures', *Proc. 10th world conf. earthquake eng.*, Madrid, Vol. 1, 1992, pp. 375–380.
3. Japan Meteorological Agency, *Earthquake Observer Guide*, 1991 (in Japanese).

4. W. B. Joyner and D. M. Boore, 'Peak horizontal acceleration and velocity from strong motion records including records from 1979 Imperial Valley, California, earthquake', *Bull. seism. soc. Am.* **71**, 2011–2038 (1981).
5. N. N. Ambraseys and J. J. Bommer, 'The attenuation of ground accelerations in Europe', *Earthquake eng. struct. dyn.* **20**, 1179–1202 (1991).
6. K. W. Campbell, 'Near-source attenuation of peak horizontal acceleration', *Bull. seism. soc. Am.* **71**, 2039–2070 (1981).
7. Y. Fukushima and T. Tanaka, 'A new attenuation relation for peak horizontal acceleration of strong earthquake ground motion in Japan', *Bull. seism soc. Am.* **80**, 757–783 (1990).
8. M. Niazi and C. P. Mortgat, 'Attenuation of peak ground acceleration in central California from observations of the 17 October 1989 Loma Prieta earthquake', *Earthquake eng. struct. dyn.* **21**, 493–507 (1992).
9. F. Yamazaki, 'The January 15, 1993 Kushiro–Oki earthquake — a quick look report', *INCEDE Newsletter*, Vol. 1 (Suppl.) 1–8 (1992).
10. The National Research Institute for Earth Science and Disaster Prevention Science and Technology Agency, 'February 7, 1993 Off Noto Peninsula earthquake', *Prompt Report on strong-motion accelerograms*, Vol. 42, 1993 (in Japanese).
11. F. Yamazaki, K. Meguro and T. Katayama, 'A quick look report on the Hokkaido-Nansai–Oki earthquake, July 12, 1993', *INCEDE Newsletter* (special issue) 1–12 (1993).
12. J. Penzien and M. Watabe, 'Characteristics of 3-dimensional earthquake ground motions', *Earthquake eng. struct. dyn.* **3**, 365–373 (1975).
13. T. Kubo and J. Penzien, 'Analysis of 3-dimensional strong ground motions along principal axes, San Fernando Earthquake', *Earthquake eng. struct. dyn.* **7**, 265–278 (1979).
14. K. Kawashima, K. Aizawa and K. Takahashi, 'Effects of composition of two horizontal components on attenuation of maximum earthquake ground motions and response spectra', *Proc. Japan soc. civil. eng.* **329**, 49–56 (1983) (in Japanese).
15. C. H. Loh, 'Analysis of the spatial variation of seismic waves and ground movements from SMART-1 array data', *Earthquake eng. struct. dyn.* **13**, 561–581 (1985).
16. T. Katayama, F. Yamazaki, S. Nagata, L. Lu and T. Turker, 'A strong motion database for the Chiba seismometer array and its engineering analysis', *Earthquake eng. struct. dyn.* **19**, 1089–1106 (1990).
17. I. A. Berensev, K.-L. Wen and Y. T. Yeh, 'Source, path and site effects on dominant frequency and spatial variation of strong ground motion recorded by SMART1 and SMART2 arrays in Taiwan', *Earthquake eng. struct. dyn.* **23**, 583–597 (1994).
18. N. M. Newmark and W. J. Hall, 'Seismic design criteria for nuclear reactor facilities', *Proc. 4th world conf. earthquake eng.*, Santiago, Chile, Vol. 2 (B4) 1969, pp. 37–50.
19. W. B. Joyner and D. M. Boore, 'Measurement, characterization and prediction of strong ground motion', *Proc. earthquake eng. soil dyn.*, Park City, ASCE, 1988, pp. 43–102.
20. J. Boatwright and D. M. Boore, 'Analysis of the ground accelerations radiated by the 1980 Livermore Valley earthquakes for directivity and dynamic source characteristics', *Bull. seism. soc. Am.* **72**, 1843–1865 (1982).
21. R. Araya and A. Der Kiureghian, 'Seismic hazard analysis including source directivity effect', *Proc. 3rd US nat. conf. earthquake eng.* Charleston, SC, Vol. 1, 1986, pp. 269–280.
22. P. Suhadolc and C. Chiaruttini, 'A theoretical study of the dependence of the peak ground acceleration on source and structure parameters', in M. O. Erdik and M. N. Toksoz (eds), *Strong Ground Motion Seismology*, Rediel, Dordrecht, 1987, pp. 143–183.
23. P. Somerville and R. Graves, 'Conditions that give rise to unusually large long period ground motions', *Struct. des. tall buildings* **2**, 211–232 (1993).